1-1-2020

# Design, Modeling and Control of a 3D Printed Monolithic Soft Robotic Finger with Embedded Pneumatic Sensing Chambers

Charbel Tawk
charbel@uow.edu.au

Hao Zhou
*University of Wollongong*, hzhou@uow.edu.au

Emre Sariyildiz
*University of Wollongong*, emre@uow.edu.au

Marc in het Panhuis
*University of Wollongong*, panhuis@uow.edu.au

Geoffrey M. Spinks
*University of Wollongong*, gspinks@uow.edu.au

*See next page for additional authors*

# Design, Modeling and Control of a 3D Printed Monolithic Soft Robotic Finger with Embedded Pneumatic Sensing Chambers


## Abstract

IEEE This paper presents a directly 3D printed soft monolithic robotic finger with embedded soft pneumatic sensing chambers (PSC) as position and touch sensors. The monolithic finger was fabricated using a low-cost and open-source fused deposition modeling (FDM) 3D printer that employs an off-the-shelf soft and flexible commercially available thermoplastic polyurethane (TPU). A single soft hinge with an embedded PSC was optimized using finite element modeling (FEM) and a hyperelastic material model to obtain a linear relationship between the internal change in the volume of its PSC and the corresponding input mechanical modality, to minimize its bending stiffness and to maximize its internal volume. The soft hinges with embedded PSCs have several advantages, such as fast response to very small changes in their internal volume (~0.0026ml/°), linearity, negligible hysteresis, repeatability, reliability, long lifetime and low power consumption. Also, the flexion of the soft robotic finger was predicted using a geometric model for use in real-time control. The real-time position and pressure/force control of the soft robotic finger were achieved using feedback signals from the soft hinges and the touch PSC embedded in the tip of the finger. This study contributes to the development of seamlessly embedding optimized sensing elements in the monolithic topology of a soft robotic system and controlling the robotic system using the feedback data provided by the sensing elements to validate their performance.



## Disciplines

Engineering | Physical Sciences and Mathematics

## Publication Details

Tawk, C., Zhou, H., Sariyildiz, E., in het Panhuis, P., Spinks, G. & Alici, G. (2020). Design, Modeling and Control of a 3D Printed Monolithic Soft Robotic Finger with Embedded Pneumatic Sensing Chambers. IEEE/ASME Transactions on Mechatronics, Online First



## Authors

Charbel Tawk, Hao Zhou, Emre Sariyildiz, Marc in het Panhuis, Geoffrey M. Spinks, and Gursel Alici

# Design, Modeling and Control of a 3D Printed Monolithic Soft Robotic Finger with Pneumatic Self-Sensing Chambers

Charbel Tawk, Hao Zhou, Emre Sariyildiz, Marc in het Panhuis, Geoffrey M. Spinks and Gursel Alici*

***Abstract*—This paper presents a directly 3D printed soft monolithic robotic finger with embedded soft self-sensing pneumatic chambers as position and touch sensors. The finger was fabricated in one manufacturing step using a low-cost and open-source fused deposition modeling (FDM) 3D. A single self-sensing hinge was optimized using finite element modeling and an experimentally identified hyperelastic material model. These self-sensing hinges have several advantages such as fast response to very small changes in their internal volume (~0.0026ml/°), linearity, negligible hysteresis, repeatability, reliability and long lifetime. In addition, the flexion of the soft robotic finger was predicted using a geometric model for use in real-time control. The real-time position and pressure/force control of the soft robotic finger were achieved using feedback signals from the soft pneumatic self-sensing hinges and touch pressure sensor embedded in the tip of the finger. This study contributes to the development of seamlessly embedding optimized sensing elements in the monolithic topology of a soft robotic system and controlling the robotic system using the feedback data provided by the sensing elements.**

***Index Terms*—Monolithic robotic system, soft robot control, soft robotic finger, soft sensors, pneumatic chambers, 3D printing.**

## I. Introduction

In recent years, the soft robotics field has received tremendous attention during which many untethered soft robots have been developed [1]. Soft robots are made of highly compliant and deformable materials which make them ideal to operate safely alongside humans and in highly dynamic environments. Ideally, an entirely soft robot must be made of soft and compliant structure, actuators, sensors, power sources and electronics [2].

Soft robots require robust soft sensors that can sustain large deformations repeatedly over long periods of time. These soft sensors are essential to develop reliable and robust control systems for soft robots. Several types of soft sensors have been developed based on different technologies for use and integration in soft robotic structures and systems including resistive strain sensors such as flex sensors [3, 4], conductive inks [5-7], ionic conductive liquids [8], liquid metals [9-11] fabrics and textiles [12,13], resistive 3D printable thermoplastics [14] and ultra-thin piezoresistive sensors [15,16]. In addition, capacitive soft sensors were established as pressure sensors [17,18], tactile sensors [19], and strain sensors [20] for various soft robotic applications including commercial wearable soft sensors [21]. Also, optical sensors were developed for use in soft prosthetic hands as strain, curvature, texture and force sensors [22]. These types of sensors developed for soft robotic systems are usually limited by hysteresis, drift over time, short lifetime, slow response or complex manufacturing methods that require multiple and laborious fabrication steps.

As an alternative, soft pneumatic chambers have been evaluated for use as soft and deformable sensors. Kong et. al [23] developed an air bladder that can be integrated into a shoe for human gait monitoring by winding a soft silicone tube that is connected to a pressure sensor. Yang et. al [24] fabricated a silicone pneumatic soft sensor based on conventional molding techniques for measuring contact forces and curvature in a soft robotic gripper. Choi et. al [25] developed a soft three-axis force sensor using radially symmetric pneumatic chambers based on the same manufacturing techniques in [24]. Gong et. al [26] used a commercially available latex tube along with pressure sensors to fabricate a tactile soft sensor for co-operative robots.

Manuscript received June, --, 2019.

This research has been supported by ARC Centre of Excellence for Electromaterials Science (Grant No. CE140100012) and the University of Wollongong, Australia.

C. Tawk and Hao Zhou are with the School of Mechanical, Materials, Mechatronic and Biomedical Engineering, and the ARC Centre of Excellence for Electromaterials Science, University of Wollongong, AIIM Facility, NSW, 2522, Australia (e-mail: ct887@uowmail.edu.au; hzhou@uow.edu.au).

E. Sariyildiz is with the School of Mechanical, Materials, Mechatronic and Biomedical Engineering, University of Wollongong, NSW, 2522, Australia (e-mail: emre@uow.edu.au)

M. in het Panhuis is with the School of Chemistry and Molecular Science and Intelligent Polymer Research Institute, ARC Centre of Excellence for Electromaterials Science, University of Wollongong, AIIM Facility, NSW, 2522, Australia (e-mail: panhuis@uow.edu.au).

G. M. Spinks is with the Intelligent Polymer Research Institute, the ARC Centre of Excellence for Electromaterials Science, University of Wollongong, AIIM Facility, NSW, 2522, Australia (e-mail: gspinks@uow.edu.au).

G. Alici is with the School of Mechanical, Materials, Mechatronic and Biomedical Engineering, and the ARC Centre of Excellence for Electromaterials Science, University of Wollongong, AIIM Facility, NSW, 2522, Australia (*Corresponding Author, e-mail: gursel@uow.edu.au.)

Slyper et. al [27] designed several building blocks that can generate various modes of deformation such as bending and twisting using 3D printing and pressure sensors. The blocks were used to rapidly prototype interactive robot skins. Vásquez et. al [28] developed 3D printed pneumatic controls based on the same printing method that can be used for haptic feedback applications. These pneumatic chambers were fabricated using high-cost 3D printers that employ soft materials with limited performance, conventional casting and molding techniques [29] or commercially available soft elastomer tubes. There are other manufacturing techniques such as fused deposition modeling (FDM) 3D printing [30-33], stereolithography [34], silicone 3D printing [35,36] and multi-material 3D printing [37-39] for fabricating soft pneumatic actuators and chambers.

Due to the control performance limitations in soft robotics, almost all robotic hands in the market are based on conventional rigid mechanisms [40]. These robotic systems require complex mechanisms and laborious assembly processes since they are made of numerous components. Moreover, their complex control algorithms require various sensors to ensure safe interaction with their environment. In contrast, soft robotic systems typified by a soft finger in this study can be directly fabricated as monolithic structures seamlessly housing soft sensors using additive manufacturing techniques where minimal or no assembly is needed. This fabrication approach makes the soft robotic systems cost-effective, customizable and lightweight compared to conventional robotic systems [41, 42].

In this work, we present a tendon-driven soft monolithic robotic finger embedded with soft pneumatic self-sensing hinges for position sensing and soft touch chambers for mechanical pressure sensing that was 3D printed in one manufacturing step without requiring any postprocessing and using a low-cost and open-source 3D printer. This work combines the soft robotic principles involved in developing robotic hands [40] and soft sensing pneumatic chambers connected to low-profile and inexpensive pressure sensors [43]. The design of a single hinge was optimized using finite element modeling (FEM) to obtain a linear relationship between the internal change in its volume and the input mechanical modality, to minimize its bending stiffness and to maximize its internal volume. A hyperelastic material model was developed for use in FEM analysis based on the stress-strain data of the soft thermoplastic poly(urethane) (TPU) used to 3D print the finger. These soft self-sensing hinges have several advantages such as fast response to a minimum change (~0.0026ml/°) in their internal volume, linearity, negligible hysteresis,

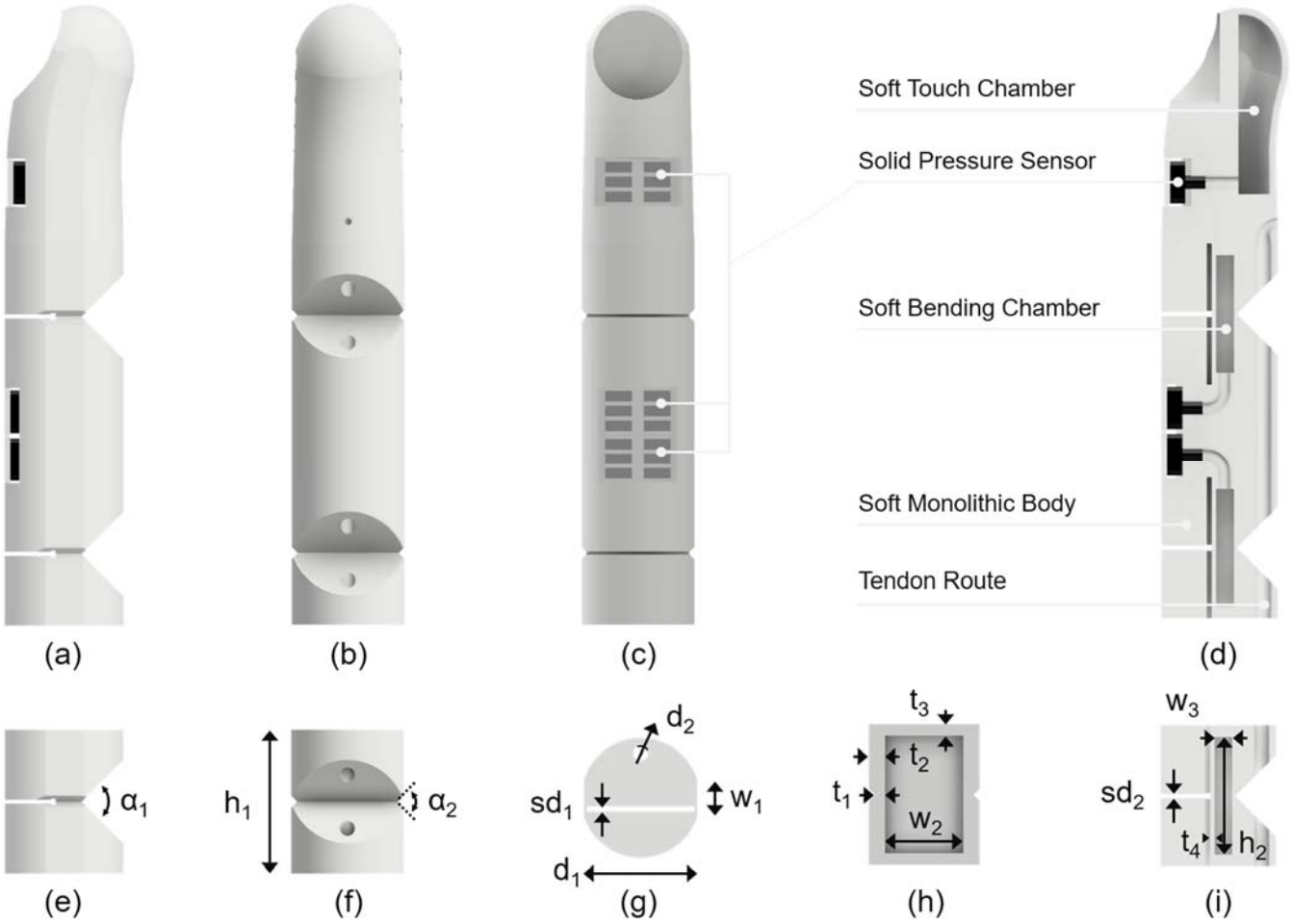


Fig. 1. 3D printed soft monolithic robotic finger with self-sensing pneumatic chambers (a) side view, (b) front view, (c) back view and (d) cross-sectional view. A single self-sensing hinge (e) side view, (f) front view, (g) top view, (h) back view cross-sectional view and (i) side view cross-sectional view. Dimensions: $\alpha_1$: 90°, $\alpha_2$: 90°, $h_1$: 24.0, $h_2$: 20.0, $sd_1$: 0.80, $sd_2$: 0.60, $d_1$: 20.0, $d_2$: 2.50, $w_1$: 6.24, $w_2$: 13.40, $w_3$: 3.0, $t_1$: 1.80, $t_2$: 2.80, $t_3$: 2.0, $t_4$: 0.80. The thickness of the touch chamber thin wall is 1.20. All dimensions are in mm.

repeatability, reliability and long lifetime. The flexion of the soft robotic finger at its joints or hinges is represented by a geometric model for use in real-time control. The real-time position and pressure/force control of the soft robotic finger were achieved using feedback signals from the soft pneumatic self-sensing hinges and touch pressure sensor. The results demonstrated in this work can be extended to other soft robotic systems where position and force feedback control systems are required. Moreover, lightweight, low-cost and low foot-print soft robotic hands can be developed based on the soft robotic finger proposed in this study.

The primary contributions of this paper are to (i) design directly 3D printed monolithic soft robotic finger with embedded self-sensing pneumatic chambers, (ii) employ a low cost and single step 3D printing technique using an off-the-shelf soft material to print the robotic finger, (iii) characterize the soft self-sensing chambers to quantify their performance (iv) develop an accurate geometric model for the underactuation of the soft robotic finger and (v) control the position and the pressure/force of the soft robotic finger based on the feedback data provided by the self-sensing pneumatic chambers embedded in the finger.

The remainder of this paper is organized as follows. Section II presents the fabrication technique, its parameters, and the characterization of the off-the-shelf printable soft material. Also, it presents the experimental hardware for the characterization and control experiments. Section III presents the finite element modeling of a single self-sensing pneumatic hinge. Section IV presents the characterization of a self-sensing pneumatic hinge in terms of linearity, hysteresis, repeatability, stability over time and lifetime. Section V presents the geometric model of the soft robotic finger. Section VI presents the position and force control experiments for the soft robotic finger. Section VII presents a discussion on the soft robotic finger and the soft pneumatic chambers. Finally, section VIII presents conclusions and future work.

## II. Soft Robotic Finger Design

### A. Modeling and Fabrication

The soft self-sensing hinges and the monolithic robotic finger were designed and modeled in Autodesk Fusion 360 (Autodesk Inc.). The minimum wall thickness of the embedded soft chambers considered during the design process was 0.8mm which is needed to ensure that the 3D printed soft chambers are airtight. The dimensions of the self-sensing hinge and the monolithic robotic finger are shown in Fig. 1. The 3D computer-aided-design (CAD) models were sliced in Simpilify3D (Simplify3D Inc.). The printing parameters were optimized and adjusted to obtain airtight soft pneumatic chambers based on our recent studies [32,43-45]. Table I. lists all the optimized parameters used to print the soft hinges and the soft robotic finger. A low-cost and open-source FDM 3D printer (FlashForge Creator Pro, FlashForge Corporation, China) was used to print the soft hinges and the soft finger using a commercially available TPU known as NinjaFlex (NinjaTek, USA).

TABLE I
TPU OPTIMIZED PARAMETERS IN SIMPLIFY 3D FOR PRINTING SOFT ROBOTIC FINGERS WITH SELF-SENSING PNEUMATIC CHAMBERS.

| Parameter | Value | Unit |
|---|---|---|
| **Resolution Settings** | | |
| Primary Layer Height | 0.1 | mm |
| First Layer Height | 0.09 | mm |
| First Layer Width | 0.125 | mm |
| Extrusion Width | 0.4 | mm |
| **Ooze Control** | | |
| Coast at End | 0.2 | mm |
| **Retraction Settings** | | |
| Retraction Length | 4 | mm |
| Retraction Speed | 40 | mm/s |
| **Speed Settings** | | |
| Default Printing Speed | 10 | mm/s |
| Outline Printing Speed | 8 | mm/s |
| Solid Infill Speed | 8 | mm/s |
| First Layer Speed | 8 | mm/s |
| X/Y Axis Movement Speed | 50 | mm/s |
| Z Axis Movement Speed | 20 | mm/s |
| **Temperature Settings** | | |
| Printing Temperature | 240 | °C |
| Heat Bed Temperature | 32 | °C |
| **Cooling Settings** | | |
| Fan Speed | 100 | % |
| **Infill Settings** | | |
| Infill Percentage | 0 | % |
| Infill/Perimeter Overlap | 30 | % |
| **Thin Walls** | | |
| Allowed Perimeter Overlap | 15 | % |
| External Thin Wall Type | Perimeters Only | - |
| Internal Thin Wall Type | Allow Single Extrusion Fill | - |
| **Movements Behavior** | | |
| Avoid Crossing Outline | ENABLED | - |
| **Additional Settings** | | |
| Extrusion Multiplier | 1.15 | - |
| Top Solid Layers | 12 | - |
| Bottom Solid Layers | 12 | - |
| Outline/Perimeter Shells | 5 | - |
| Wipe Nozzle | DISABLED | - |
| **Support Material Generation** | | |
| Support Type | From Build Platform Only | - |

### B. TPU Characterization and Material Model

An experimental uniaxial tensile test was performed on 16 TPU samples to extract the stress-strain behavior of the TPU. Eight TPU samples were printed using a longitudinal infill pattern to assess the effect of different infill patterns on the behavior of the TPU. The remaining samples were printed using a crosswise infill pattern. The two infill patterns had an insignificant effect on the average tensile data of the TPU. The tests were conducted on the TPU samples according to the ISO 37 standard where all the samples were stretched by 800% at a rate of 100mm/s using an electromechanical Instron Universal Testing machine (Instron8801). The average stress-strain data shown in Fig. 2. was used to develop a 5-Parameter Mooney-Rivlin hyperelastic material model in ANSYS (Release 19.1, ANSYS, Inc.). The model was implemented for use in finite element simulations. The parameters of the material model are listed in Table II.

TABLE II
TPU HYPERELASTIC MATERIAL MODEL CONSTANTS

| Hyperelastic Material Model | Material Constant | Value |
|---|---|---|

| | | |
|---|---|---|
| **Mooney Rivlin** | C10 | -0.233 MPa |
| | C01 | 2.562 MPa |
| | C20 | 0.116 MPa |
| | C11 | -0.561 MPa |
| | C02 | 0.900 MPa |
| | Incompressibility Parameter D1 | 0.000 $MPa^{-1}$ |

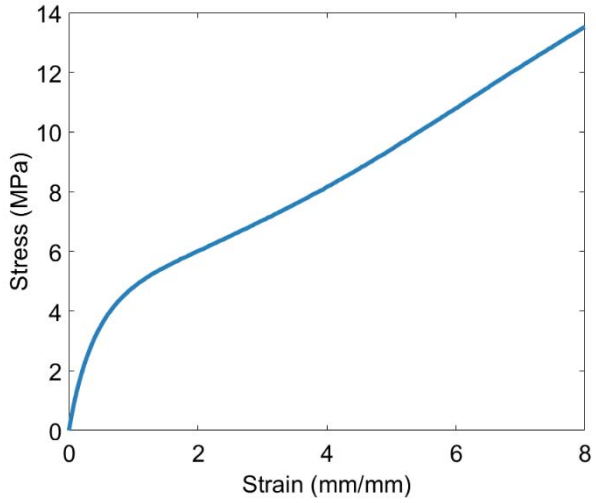


Fig. 2. TPU average stress-strain data.

### C. Experimental Hardware and Setup

Analog pressure sensors (ABPDANT015PGAA5, 0 to 15 psi Gauge, 0.25% accuracy, Honeywell International Inc.) were used to detect the minimum volume change (~0.0026ml/°), in the embedded 3D printed soft chambers. An Arduino UNO microcontroller was used to characterize the performance of the soft hinges. Simulink® Desktop Real-Time of Matlab (The MathWorks, Inc.), a data acquisition card (Humusoft MF644, HUMUSOFT s.r.o.), a brushless DC motor (Maxon EC-i40, GP42C planetary gearhead with 91:1 reduction ratio, maxon motor ag, Switzerland), a motor driver (ESCON 50/5, maxon motor ag, Switzerland), and a quadrature encoder (ENX 16 EASY Encoder with 1024 counts per turn, maxon motor ag, Switzerland) were used to perform real-time control experiments. A commercially available thin and flexible fishing line (46.6kg/dia:0.483mm, GRAND PE WX8, JIGMAN, Japan) was used as a tendon to drive the soft robotic finger.

### D. Finite Element Modeling

The design of a single self-sensing hinge was optimized using FEM to obtain a linear relationship between the change in its internal volume and the input mechanical deformation, minimize its bending stiffness and maximize its internal volume. Ideally, a relationship exists between the change in the internal volume of the soft internal chamber and the experimental pressure change ($P_1V_1 = P_2V_2$) obtained due to the mechanical deformation applied. Fig. 3. shows that the initial design of the hinge produced a nonlinear relationship between the change in volume and the bending angle. However, successive improvements and modification to the finger design ultimately produced a linear relationship between the change in volume and the bending angle (Fig. 4.). This final design is as shown in Fig. 1. The wall thickness ($t_2$) was found to be the main critical parameter affecting the linearity of the relationship between bend angle and volume change. The wall thickness of the side walls ($t_2$) had to be large enough compared to the wall thickness of the thin wall ($t_4$) to prevent the side walls from deforming inward toward each other when the hinge is bent. Also, the separation of the thin wall ($t_4$) from the back part of the hinge ($sd_1$) was critical to achieve linearity. The thin wall should be free from any constraints along its length. In addition, the thickness of the side walls ($t_2$) was increased to minimize the bending stiffness of the joint. Thicker side walls result in a higher bending stiffness. In addition, the upper and lower parts of the hinge were separated ($sd_2$) to further reduce the bending stiffness. The models were meshed using higher order tetrahedral elements. In terms of boundary conditions, a fixed support was applied at the base of the soft hinge and a displacement support normal to the base of the hinge was applied at the base of the tendon. A displacement of 12.0mm was applied. Moreover, frictional and bonded contact pairs were defined. A frictional and symmetric contact pair was defined between the internal walls of the soft chamber. A similar contact pair was defined between the outer walls of the hinge that come in contact upon full closure. Another frictional and symmetric contact pair was defined between the bottom hole of the hinge and the tendon. Additionally, a bonded contact pair was defined between the top hole of the hinge and the tendon.

The minimum and maximum running times of the FEM simulations for the final design are 119s (≈1.98min) and 1000s (≈16.67min), respectively. It is important to note that the simulation time can be significantly decreased by allocating more memory. The only challenges encountered were the distortion of some elements due to the large mechanical deformations and the contact between the soft hinge and the tendon. However, this issue was alleviated by incorporating a coarser mesh for the hinge that is suitable for hyperelastic materials and a finer mesh for the tendon. The mesh used was selected to verify that the results are accurate and not affected by the mesh size. Therefore, finite element modeling can be used to predict the behavior of the self-sensing hinges and to optimize their topology to meet specific design requirements quickly and efficiently prior to developing physical prototypes.

## III. Characterization of Soft Robotic Finger

A single optimized self-sensing pneumatic hinge was characterized to assess its performance in terms of linearity, hysteresis, repeatability, reliability, stability over time and lifetime.

### A. Linearity and Hysteresis

A single self-sensing hinge was activated to assess its linearity and hysteretic behavior. The input mechanical deformation was ramped up and down using a step angle of 10°. Fig. 5. shows that there is a linear relationship between the output pressure and the input mechanical deformation. In addition, Fig. 5. shows that the hinge has a negligible hysteresis. These features, linearity and negligible hysteresis, are essential for the implementation of direct and simple linear control systems.

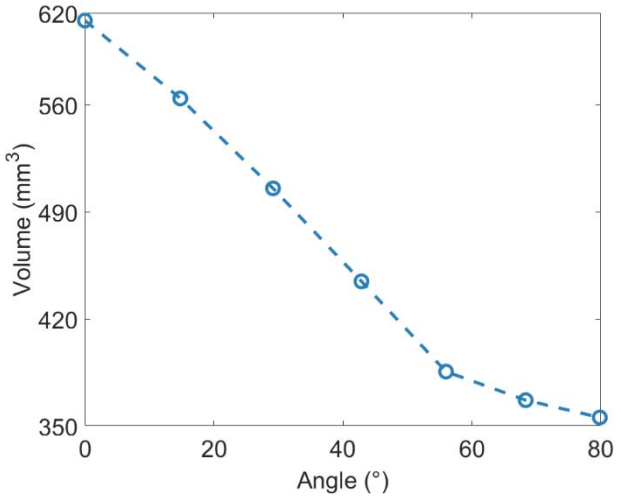


Fig. 3. Volume change versus bending angle for the initial self-sensing hinge design.

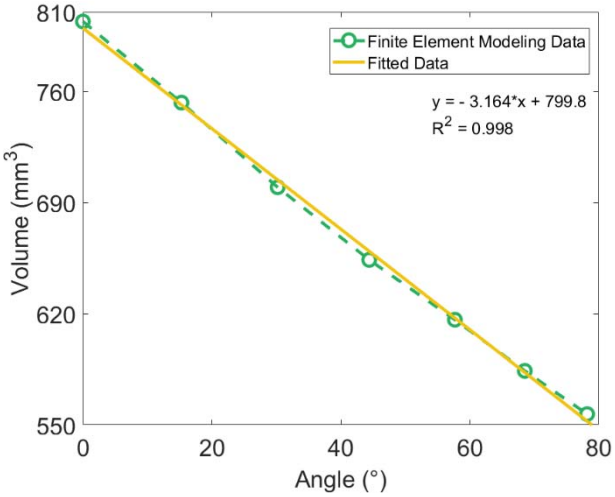


Fig. 4. Volume change versus bending angle for the optimized (i.e. final) self-sensing hinge design, that is illustrated in Fig. 1.

### *B. Repeatability and Reliability*

A single self-sensing hinge was activated repeatedly for 600 cycles (i.e. 10 minutes) with an activation frequency of 1.0 Hz to assess its repeatability and reliability. In each activation cycle, the hinge was fully closed. Fig. 6. shows that the hinge generated a consistent and repeatable signal. However, there was a slight change in the pressure upon recovery as shown in Fig. 7. The main reason for this change is that the hinge did not have enough time to recover its initial shape due to the material properties of the TPU. Although NinjaFlex is soft and flexible, it cannot recover its initial shape as fast as soft silicones when thick structures are involved.

### *C. Drift Over Time*

A single self-sensing hinge was fully closed for a period of 30 minutes while its internal pressure was monitored to check for any drift over time. The pressure changed by 2.41% during the actuation period as shown in Fig. 8. There are two main reasons for this slight change over time. First, when the hinge was fully closed, the tendon was loosened slightly due to the stretch and relaxation of the TPU at the hole of the hinge where the tendon is running. Second, a slight leakage from the fittings and connectors used was noticed. These effects had only a

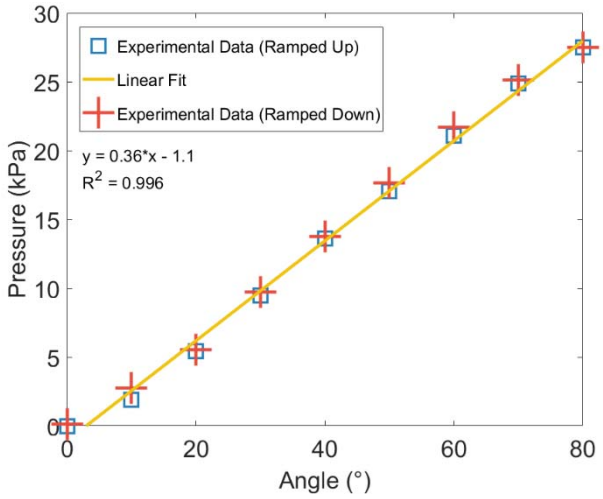


Fig. 5. Self-sensing pneumatic hinge linearity and hysteresis experimental results.

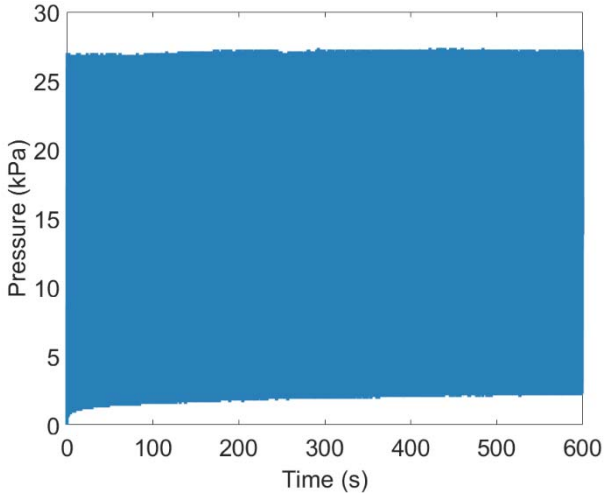


Fig. 6. The repeatability of the pressure change of the self-sensing pneumatic hinge for 600 bending cycles.

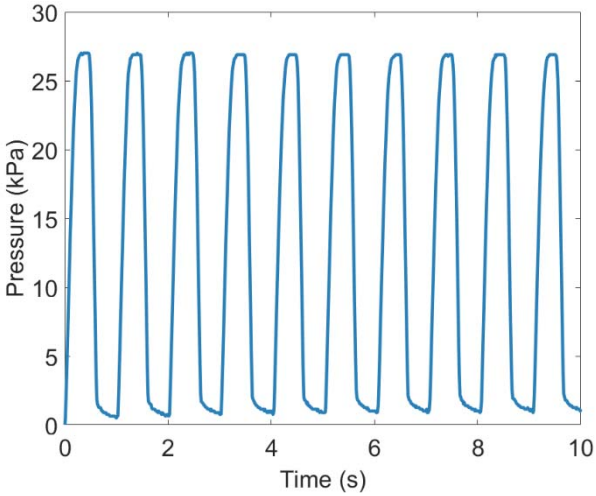


Fig. 7. The repeatability of the pressure change of the self-sensing pneumatic hinge for typical 10 bending cycles.

minor influence on the holding pressure, which is promising as pressure stability is essential to develop reliable control systems for soft robotic systems.

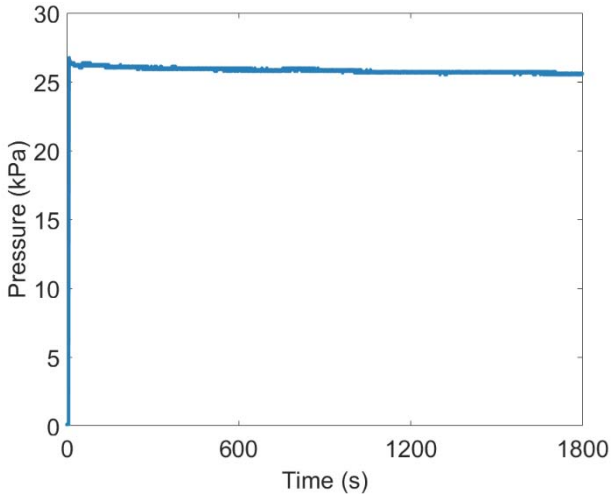


Fig. 8. The pressure stability of the self-sensing hinge over time.

### D. Lifetime

A single self-sensing pneumatic hinge was activated repeatedly with a frequency of 1.0 Hz to assess its lifetime. In each cycle, the hinge was fully closed and relaxed. The hinge sustained 100,000 cycles without failure and any degradation in performance. In a previous study [42], we showed that a similar flexure hinge without pneumatic chambers can sustain more than 1.5 million cycles without any degradation in performance or structural damage. Therefore, these self-sensing hinges are ideal for reliable soft robotic applications such as soft robotic hands, soft prosthetic hands and soft adaptive grippers that require repeatable deformations over sustained periods of time.

## IV. Soft Robotic Finger Modeling

The soft robotic finger can be modeled using the direct relationship between the output pressure and the angular displacement for each joint (Fig. 9.) with reference to the experimental result in Fig. 5. The angular position of each joint can be obtained directly from the corresponding pressure readings as follows:

$$\theta_1 = \alpha_1 P_1 + \beta_1 \quad (1)$$

$$\theta_2 = \alpha_2 P_2 + \beta_2 \quad (2)$$

where $\theta_1$ is the angular position of Hinge 1, $\theta_2$ is the angular position of Hinge 2, $P_1$ is the pressure for Hinge 1, $P_2$ is the pressure for Hinge 2, and $\alpha_1, \beta_1, \alpha_2$ and $\beta_2$ are the constants of the linear model which are experimentally identified to be 2.6548, -5.5752, 2.4931 and -4.9861 °/kPa, respectively.

A geometric model can be derived (Fig. 9.) to obtain a relationship between the change in the length of the tendon at each joint and the corresponding bending angle as follows:

$$L_1 = L\sqrt{2(\cos({}^{\pi}/_{2} - \theta_1)} \quad (3)$$

$$L_2 = L\sqrt{2(\cos({}^{\pi}/_{2} - \theta_2)} \quad (4)$$

where $L_1$ is the length of the tendon at an arbitrary position at Hinge 1, $L_2$ is the length of the tendon at the same arbitrary position at Hinge 2 and $L$ is the distance between the tendon and the pivot point of each hinge.

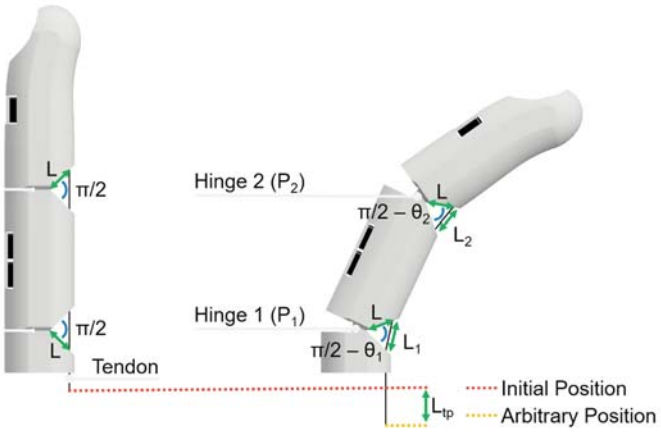


Fig. 9. The geometric model parameters for the soft robotic finger.

The total change in the length of the tendon, $L_{tp}$, based on the model of the pressure sensors can be written as follows:

$$L_{tp} = L_1 + L_2 \quad (5)$$

The total change in the length of the tendon, $L_{te}$, can also be derived based on the data obtained from the quadrature encoder as follows:

$$L_{te} = r_p \theta_e \quad (6)$$

where $r_p$ is the radius of the pulley to which the tendon is attached and $\theta_e$ is its corresponding angular displacement of the motor as measured by the encoder.

The angular displacements $\theta_{tp}$ and $\theta_{te}$ can be expressed as follows:

$$\theta_{tp} = {}^{L_{tp}}/_{r_p} \quad (7)$$

$$\theta_e = {}^{L_{te}}/_{r_p} \quad (8)$$

where $r_p = 40mm$.

## V. Soft Robotic Finger Control

The real-time position and pressure/force control experiments of the soft robotic finger were conducted using a quadrature encoder and the soft pneumatic self-sensing hinges. Proportional, Integral, Derivative (PID) and PI controllers were employed to perform the position and pressure/force control experiments, respectively. The PID control gains were tuned experimentally.

### A. Position Control Based on Quadrature Encoder

The change in the length of the tendon obtained from the geometric model (i.e. angular displacement, Eq. 7.) was compared with the change in the length of the tendon obtained from the model of the encoder (Eq. 8.). A trajectory tracking control experiment was conducted with an amplitude of pi/17 (i.e. which corresponds to the length of the tendon, Eqs. 7 and 8) and a frequency of 1.0 Hz. The feedback control signal is obtained from the encoder. Fig. 10. shows that the motor can precisely follow the position reference when the encoder feedback is used (i.e. it is the expected result with the PID controller with the gains of $k_p = 250$, $k_i = 5$ and $k_d = 10$.

More importantly, the measurement from the pneumatic sensors is verified with this experiment. The length of the cable (i.e. angle of the pulley) can be precisely estimated by using the proposed sensors and their corresponding geometric model (Eqs. 1-5) as shown in Fig. 10. and Video S1. The block diagram of the control loop is shown in Fig. 11.

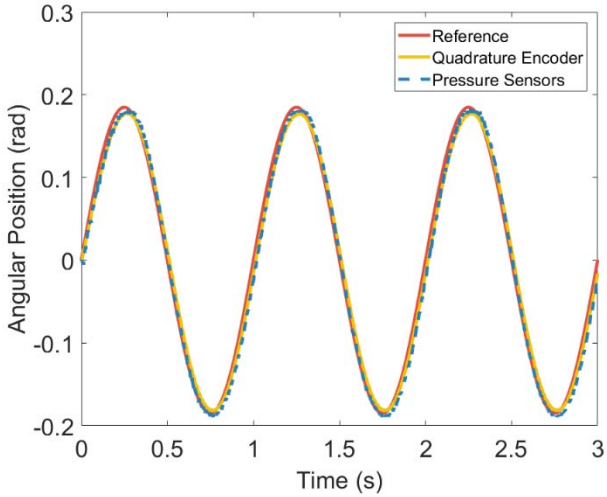


Fig. 10. Experimental results verifying the performance of the sensing pressure chambers, which provide the joint angle data to correctly estimate the tendon length from Eqs. 5 and 7. The control signal was provided by the motor encoder. Please note the close match between the encoder readings and the corresponding readings of the sensing pressure chambers.

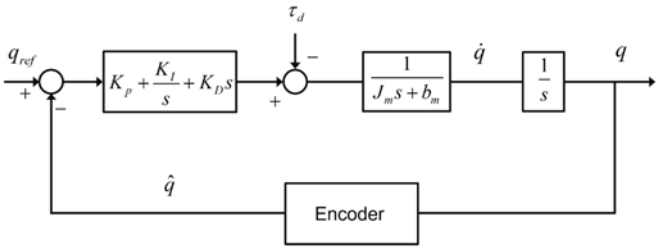


Fig. 11. Control loop block diagram for the performance verification of the sensing pressure chambers based on the feedback provided by the encoder.

### B. *Position Control Based on Geometric Model*

After the geometric model (Eqs. 5 and 7) was verified, the same trajectory tracking control experiment was performed with the same applied reference input. However, the feedback signal was obtained from the pressure sensors instead of the encoder. The most significant result in this experiment is that the motor can precisely follow the reference trajectory when the pneumatic sensors' measurements are used as shown in Fig. 12. and Video S1. Fig. 12. shows that high-performance trajectory tracking can be performed by using only the pneumatic sensors measurement under the PID controller with the gains of $k_p = 55$, $k_i = 50$ and $k_d = 1$. Also, Fig. 12 shows that the encoder signal accurately follows the pressure sensors signal which again verifies the accuracy of the geometric model. The block diagram of the control loop is shown in Fig. 13.

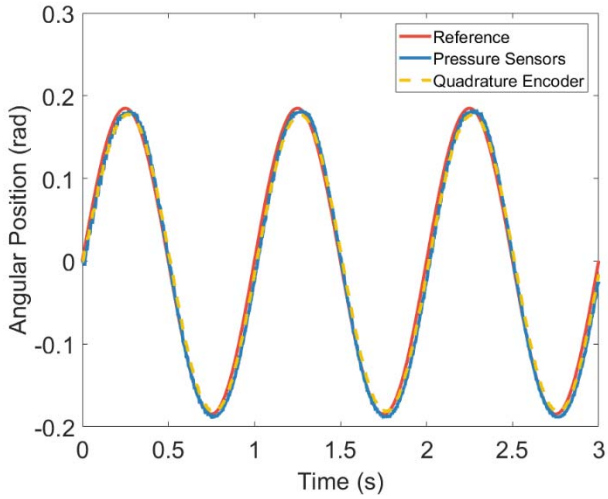


Fig. 12. Experimental results verifying the control performance of the sensing pressure chambers, which provide the joint angle feedback data to control the tendon length. The corresponding encoder readings were used to correctly estimate the tendon length from Eq. 6. Please note the close match between the readings of the sensing pressure chambers and the corresponding encoder readings.

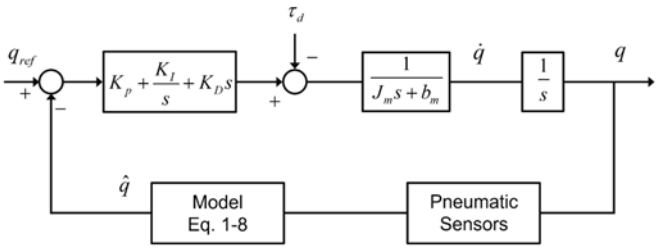


Fig. 13. Control loop block diagram for the control of the soft robotic finger based on the feedback provided by the pressure chambers.

### C. *Step Response Based on Geometric Model*

The feedback control was performed by using the pressure sensors signals where the encoder reading was used to verify the performance of the position measurement. Fig. 14. shows the step response of the soft finger using the feedback data provided by the sensing chambers embedded in the hinges. ($\approx 8.55\%$ overshoot, $29.09ms$ rise time < $72ms$ settling time) under the PID controller with the gains of $k_p = 25$, $k_i = 50$ and $k_d = 1.25$.

### D. *Force/Pressure Control*

The proposed pneumatic soft sensors can be used to estimate not only the position of hinges of the soft robotic finger but also its tip force/pressure. To this aim, a soft sensing chamber was embedded at the tip of the soft finger, as illustrated in Fig. 1. The position control was performed by using the same step reference input when there was an obstacle. The robotic finger could not follow the position reference due to the obstacle as shown in Fig. 15. The output of the pressure sensor and the estimated contact force which is obtained by an observer are illustrated in Fig. 16. This figure shows that the pressure sensor and the disturbance forces have similar characteristic curves. The block diagram of the pressure/force control loop is shown in Fig. 17.

As shown in Fig. 18, a closed-loop force control could be performed by using the soft touch sensor. The closed-loop

force/pressure control was achieved using an experimentally tuned PI controller with the gains of $k_p = 0.75$ and $k_i = 6$.

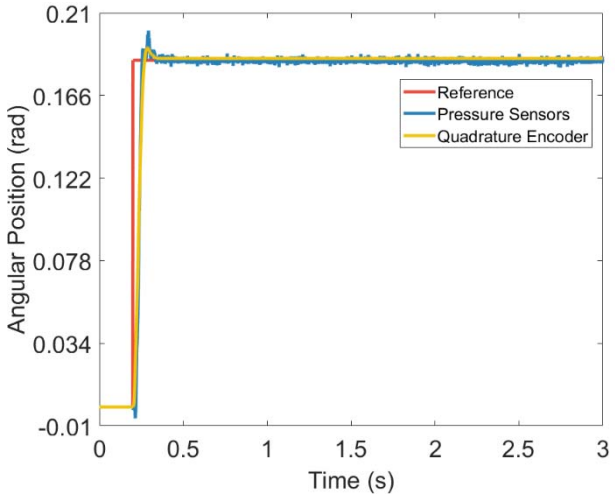


Fig. 14. Step response of the soft finger with feedback data provided by the sensing chambers embedded in its hinges.

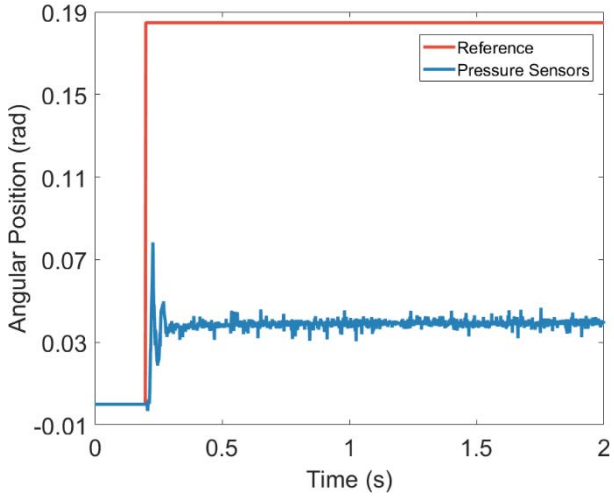


Fig. 15. Soft finger position after an obstacle was encountered.

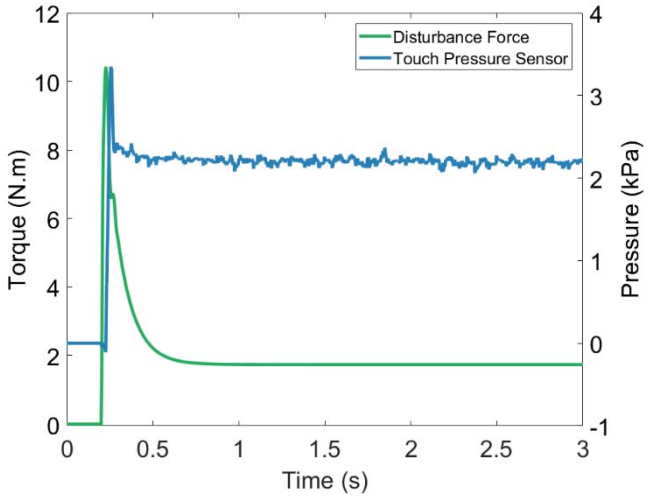


Fig. 16. Computed torque and touch sensor characteristic curves.

It was proven that soft pneumatic sensors can be modeled and used as force sensors (24,25). In this work, the main objective was to fully characterize, model and implement the proposed soft position sensors. The pressure/force sensor introduced in this section showed its potential as a force sensor.

It is important to note that only pressure control was performed (i.e., force control is not performed). In order to perform force control, the touch pressure sensor should be modeled to measure the corresponding force. This pressure control result is a preliminary result which proves that force control can be performed by using the pneumatic touch sensor embedded at the tip of the soft robotic finger. This pressure/force sensor will be comprehensively studied in future work, as stated in Section VII.

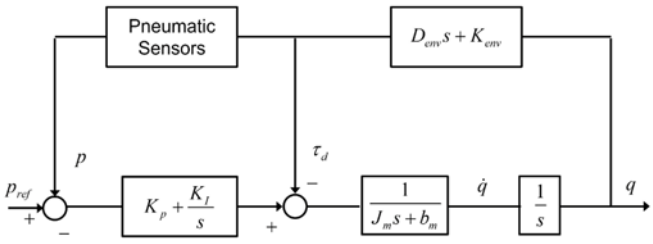


Fig. 17. Pressure/force control loop block diagram.

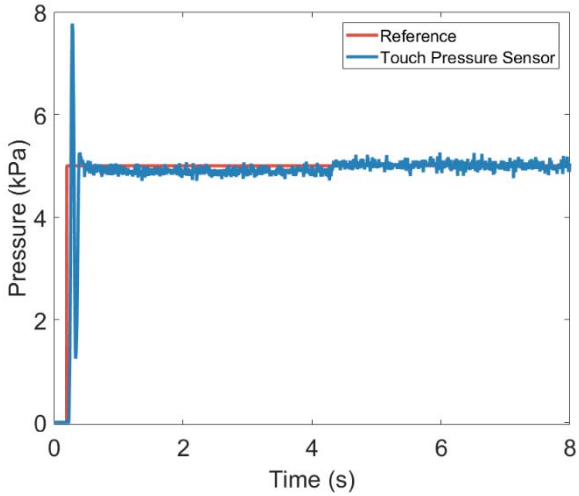


Fig. 18. Closed-loop force control based on the touch pressure sensor.

## VI. Discussion

The objective of this study is to design, fabricate, model and control a soft monolithic robotic finger with self-sensing soft pneumatic sensing chambers embedded in its hinges or joints, and to control the tip force using the touch sensing chambers embedded in the tip of the soft finger. The soft robotic finger and the soft chambers were directly fabricated as a monolithic body in one manufacturing step using a low-cost 3D printer. The self-sensing pneumatic chambers used in this study are not by themselves soft sensors (42). Commercial pressure sensors are employed to measure the pressure in the soft chambers, as shown in Fig. 1 and to control the position and force/pressure of the robotic finger. One limitation of the solid pressure sensors is their relatively noisy signal which needs to be appropriately processed before it can be used for the control purpose. The soft pneumatic self-sensing chambers can be used in soft robotic applications where soft position and force sensors are required (42). One of the aims of soft robotics is to

design and fabricate soft robotic systems with a monolithic topology embedded with its actuators and sensors such that they can safely interact with their immediate physical environment.

This study significantly contributes to the research efforts to achieve this overarching aim. The sensors are seamlessly integrated into the monolithic topology of the soft finger for the position and force control, which ideally require co-located sensors, as demonstrated in this study. In addition, our aim is to fabricate low-cost, lightweight and low-foot-print soft monolithic structures with embedded self-sensing capabilities using low-cost and open-source 3D printing technologies. In this study, we proved that these low-cost soft robotic systems can be easily and rapidly designed, modeled, fabricated and controlled which make them suitable to be directly implemented by roboticists, engineers, scientists and hobbyists in diverse robotic applications such as robotic hands, soft prosthetic hands, soft prosthetic fingers and adaptive grippers.

Finally, this work is aligned with our previous work (42) objectives such as adding reliable sensing ability to underactuated soft robotic hands at a minimum cost, reducing space usage in these soft robotic hands and eliminating the need for encoders to control the tendon driven underactuated soft robotic fingers.

## VII. Conclusion And Future Work

We have presented a monolithic soft robotic finger embedded with soft pneumatic sensing chambers that can be used for position and force control. The soft finger was 3D printed, without requiring any postprocessing, using a low-cost and open-source 3D printer. A self-sensing hinge was optimized using FEM to obtain a linear relationship between the internal change in its volume and the input mechanical deformation, to minimize its bending stiffness and to maximize its internal volume. A hyperelastic material model was developed for the 3D printed TPU based on its experimental stress-strain data. The model was implemented in FEM simulations to predict accurately the behavior of the self-sensing hinges. The monolithic self-sensing hinges have multiple advantages such as fast response to a minimum change of ~0.0026 ml/° in their internal volume due to mechanical deformations, linearity, insignificant hysteresis, repeatability, reliability and long lifetime. A geometric model for the tendon length has been proposed and experimentally verified for the real-time control and actuation of the soft robotic finger. The feedback signals from the soft pneumatic self-sensing hinges and touch pressure sensor were used to control the position and the tip force of the soft robotic finger in real-time. This work has demonstrated that these soft pneumatic self-sensing chambers can seamlessly be integrated into soft robotic systems to control their position and force. We envisage that these robotic fingers can be used in diverse applications including soft prosthetic hands, adaptive grippers, robotic hands and other similar robotic applications. In future work, the soft touch sensors will be fully characterized, modeled and studied for use as embedded touch sensors. In addition, a complete robotic hand will be developed and controlled based on the soft robotic finger embedded with soft sensing chambers as its position and force sensors.

## VIII. Acknowledgment

This research has been supported by ARC Centre of Excellence for Electromaterials Science (Grant No. CE140100012) and the University of Wollongong, Australia. The authors would like to thank Dr. Rahim Mutlu (University of Wollongong, Australia) and Mr. Aibek Niyetkaliyev (University of Wollongong, Australia) for their help to conduct the control experiments.

## References

[1] S. I. Rich, R. J. Wood, and C. Majidi, "Untethered soft robotics," *Nat. Electron.,* vol. 1, no. 2, pp. 102-112, 2018.

[2] G. Alici, "Softer is Harder: What Differentiates Soft Robotics from Hard Robotics?," *MRS Adv.,* vol. 3, no. 28, pp. 1557-1568, 2018.

[3] G. Gerboni, A. Diodato, G. Ciuti, M. Cianchetti, and A. Menciassi, "Feedback Control of Soft Robot Actuators via Commercial Flex Bend Sensors," *IEEE/ASME Trans. Mech.,* vol. 22, no. 4, pp. 1881-1888, 2017.

[4] K. Elgeneidy, N. Lohse, and M. Jackson, "Bending angle prediction and control of soft pneumatic actuators with embedded flex sensors – A data-driven approach," *Mechatronics,* vol. 50, pp. 234-247, 2018.

[5] J. T. Muth *et al.*, "Embedded 3D Printing of Strain Sensors within Highly Stretchable Elastomers," *Adv. Mater.,* vol. 26, no. 36, pp. 6307-6312, 2014.

[6] J. C. Yeo, H. K. Yap, W. Xi, Z. Wang, C.-H. Yeow, and C. T. Lim, "Flexible and Stretchable Strain Sensing Actuator for Wearable Soft Robotic Applications," *Adv. Mater. Technol.,* vol. 1, no. 3, p. 1600018, 2016.

[7] S. Kumbay Yildiz, R. Mutlu, and G. Alici, "Fabrication and characterisation of highly stretchable elastomeric strain sensors for prosthetic hand applications," *Sens. Actuators A Phys.,* vol. 247, pp. 514-521, 2016.

[8] R. L. Truby *et al.*, "Soft Somatosensitive Actuators via Embedded 3D Printing," *Adv. Mater.,* vol. 30, no. 15, p. 1706383, 2018.

[9] Y. Park, B. Chen, and R. J. Wood, "Design and Fabrication of Soft Artificial Skin Using Embedded Microchannels and Liquid Conductors," *IEEE Sens. J.,* vol. 12, no. 8, pp. 2711-2718, 2012.

[10] W. Xi, J. C. Yeo, L. Yu, S. Zhang, and C. T. Lim, "Ultrathin and Wearable Microtubular Epidermal Sensor for Real-Time Physiological Pulse Monitoring," *Adv. Mater. Technol.,* vol. 2, no. 5, p. 1700016, 2017.

[11] M. D. Dickey, "Stretchable and Soft Electronics using Liquid Metals," *Adv. Mater.,* vol. 29, no. 27, p. 1606425, 2017.

[12] M. Stoppa and A. Chiolerio, "Wearable Electronics and Smart Textiles: A Critical Review," *Sensors,* vol. 14, no. 7, p. 11957, 2014.

[13] M. C. Lina and B. F. Alison, "Smart fabric sensors and e-textile technologies: a review," *Smart Mater. Struct.,* vol. 23, no. 5, p. 053001, 2014.

[14] K. Elgeneidy, G. Neumann, M. Jackson, and N. Lohse, "Directly Printable Flexible Strain Sensors for Bending and Contact Feedback of Soft Actuators," *Front. Robot. AI,* vol. 5, no. 2, 2018.

[15] V. Sencadas, R. Mutlu, and G. Alici, "Large area and ultra-thin compliant strain sensors for prosthetic devices," *Sens. Actuators A Phys.,* vol. 266, pp. 56-64, 2017.

[16] H. Mai, R. Mutlu, C. Tawk, G. Alici, and V. Sencadas, "Ultra-stretchable MWCNT–Ecoflex piezoresistive sensors for human motion detection applications," *Compos. Sci. Technol.,* vol. 173, pp. 118-124, 2019.

[17] O. Atalay, A. Atalay, J. Gafford, and C. Walsh, "A Highly Sensitive Capacitive-Based Soft Pressure Sensor Based on a Conductive Fabric and a Microporous Dielectric Layer," *Adv. Mater. Technol.,* vol. 3, no. 1, p. 1700237, 2018.

[18] L. Viry *et al.*, "Flexible Three-Axial Force Sensor for Soft and Highly Sensitive Artificial Touch," *Adv. Mater.,* vol. 26, no. 17, pp. 2659-2664, 2014.

[19] L. Bin, G. Yang, F. Adam, and V. Yon, "Soft capacitive tactile sensing arrays fabricated via direct filament casting," *Smart Mater. Struct.,* vol. 25, no. 7, p. 075009, 2016.

[20] A. Frutiger *et al.*, "Capacitive Soft Strain Sensors via Multicore–Shell Fiber Printing," *Adv. Mater.,* vol. 27, no. 15, pp. 2440-2446, 2015.

[21] www.stretchsense.com
[22] H. Zhao, K. O'Brien, S. Li, and R. F. Shepherd, "Optoelectronically innervated soft prosthetic hand via stretchable optical waveguides," *Sci. Robot.,* vol. 1, no. 1, 2016.
[23] K. Kong and M. Tomizuka, "A Gait Monitoring System Based on Air Pressure Sensors Embedded in a Shoe," *IEEE/ASME Trans. Mech.,* vol. 14, no. 3, pp. 358-370, 2009.
[24] H. Yang, Y. Chen, Y. Sun, and L. Hao, "A novel pneumatic soft sensor for measuring contact force and curvature of a soft gripper," *Sens. Actuators A Phys.,* vol. 266, pp. 318-327, 2017.
[25] H. Choi, P. Jung, K. Jung, and K. Kong, "Design and fabrication of a soft three-axis force sensor based on radially symmetric pneumatic chambers," in *Proc. IEEE Int. Conf. Robot. Autom.*, 2017, pp. 5519-5524.
[26] D. Gong, R. He, J. Yu, and G. Zuo, "A Pneumatic Tactile Sensor for Co-Operative Robots," *Sensors,* vol. 17, no. 11, p. 2592, 2017.
[27] R. Slyper and J. Hodgins, "Prototyping robot appearance, movement, and interactions using flexible 3D printing and air pressure sensors," in *Proc. IEEE RO-MAN: The 21st IEEE International Symposium on Robot and Human Interactive Communication*, 2012, pp. 6-11.
[28] M. Vázquez *et al.*, "3D Printing Pneumatic Device Controls with Variable Activation Force Capabilities," in *Proc. of the 33rd Annual ACM Conference on Human Factors in Computing Systems*, 2015, pp. 1295-1304.
[29] A. D. Marchese, R. K. Katzschmann, and D. Rus, "A Recipe for Soft Fluidic Elastomer Robots," *Soft robot.,* vol. 2, no. 1, pp. 7-25, 2015.
[30] H. K. Yap, H. Y. Ng, and C.-H. Yeow, "High-Force Soft Printable Pneumatics for Soft Robotic Applications," *Soft Robot.*, vol. 3, no. 3, pp. 144-158, 2016.
[31] B. A. W. Keong and R. Y. C. Hua, "A Novel Fold□Based Design Approach toward Printable Soft Robotics Using Flexible 3D Printing Materials," *Adv. Mater. Technol.*, vol. 3, no. 2, p. 1700172, 2018.
[32] C. Tawk, M. in het Panhuis, G.M, Spinks, and G. Alici, "Bioinspired 3D Printable Soft Vacuum Actuators for Locomotion Robots, Grippers and Artificial Muscles", *Soft Robot.*, vol. 5, no. 6, pp. 685-694, 2018.
[33] R. Mutlu, C. Tawk, G. Alici, and E. Sariyildiz, "A 3D printed monolithic soft gripper with adjustable stiffness," in *Proc. IECON 2017 - 43rd Annual Conference of the IEEE Industrial Electronics Society*, 2017, pp. 6235-6240.
[34] N. P. Bryan, J. W. Thomas, Z. Huichan, and F. S. Robert, "3D printing antagonistic systems of artificial muscle using projection stereolithography," *Bioinspir. Biomim.*, vol. 10, no. 5, p. 055003, 2015.
[35] O. D. Yirmibesoglu et al., "Direct 3D printing of silicone elastomer soft robots and their performance comparison with molded counterparts," in *Proc. IEEE Int. Conf. Soft Robot.*, 2018, pp. 295-302.
[36] M. Schaffner, J. A. Faber, L. Pianegonda, P. A. Rühs, F. Coulter, and A. R. Studart, "3D printing of robotic soft actuators with programmable bioinspired architectures," *Nat. Commun.,* vol. 9, no. 1, p. 878, 2018.
[37] R. MacCurdy, R. Katzschmann, K. Youbin, and D. Rus, "Printable hydraulics: A method for fabricating robots by 3D co-printing solids and liquids," in *Proc. IEEE Int. Conf. Robot. Autom.*, 2016, pp. 3878-3885.
[38] Z. Wang, and S. Hirai, "Soft Gripper Dynamics Using a Line-Segment Model With an Optimization-Based Parameter Identification Method," *IEEE Robot. Autom. Lett.*, vol. 2, no. 2, pp. 624-631, 2017.
[39] D. Drotman, S. Jadhav, M. Karimi, P. deZonia, and M. T. Tolley, "3D printed soft actuators for a legged robot capable of navigating unstructured terrain," in *Proc. IEEE Int. Conf. Robot. Autom.,* 2017, pp. 5532-5538.
[40] C. L. Semasinghe, D. G. K. Madusanka, R. K. P. S. Ranaweera, and R. A. R. C. Gopura, "Transradial prostheses: Trends in development of hardware and control systems," *Int. J. Med. Robotics Comput. Assist. Surg.,* vol. 15, no. 1, p. e1960, 2019.
[41] R. Mutlu, G. Alici, M. in het Panhuis, and G. Spinks, "3D Printed Flexure Hinges for Soft Monolithic Prosthetic Fingers," *Soft Robot.,* vol. 3, no. 3, pp. 120-133, 2016.
[42] H. Zhou, A. Mohammadi, D. Oetomo, and G. Alici, "A Novel Monolithic Soft Robotic Thumb for an Anthropomorphic Prosthetic Hand," *IEEE Robot. Autom. Lett.,* vol. 4, no. 2, pp. 602-609, 2019.
[43] C. Tawk, M. in het Panhuis, G. M. Spinks, and G. Alici, "Soft Pneumatic Sensing Chambers for Generic and Interactive Human–Machine Interfaces," *Adv. Intell. Sys.,* vol. 1, no. 1, p. 1900002, 2019.
[44] C. Tawk, G. M. Spinks, M. in het Panhuis, G. Alici, "3D Printable Linear Soft Vacuum Actuators (LSOVA): their modeling, performance quantification and application in soft robotic systems," *IEEE/ASME Trans. Mech*., Accepted for publication on 25 March 2019.
[45] C. Tawk, A. Gillett, M. in het Panhuis, G. M. Spinks, and G. Alici, "3D Printed Omni-Purpose Soft Gripper," *IEEE Trans. Robot.,* In print, June 2019.

**Charbel Tawk** received his B.E. in mechanical engineering with high distinction from the Lebanese American University (LAU) in 2016. Currently, he is a PhD candidate in Soft Robotics at the University of Wollongong, Australia and the ARC Centre of Excellence for Electromaterials Science (ACES) where his research work focuses on novel 3D printable soft actuators and sensors for diverse soft robotic applications.

His research interests include 3D printed soft robots, actuators and sensors, soft and interactive human-machine interfaces and 3D printing.

**Hao Zhou** received the B.S. degree in building environment and facility engineering from Tongji University, Shanghai, China, in 2004, the M.S. degree in mechanical engineering from the University of Queensland, Brisbane, QLD, Australia, in 2008, the second M.S. degree in engineering practice (mechanical) from the University of Wollongong, Wollongong, NSW, Australia, in 2009, the Ph.D. degree from the School of Mechanical, Materials, Mechatronic and Biomedical Engineering, University of Wollongong, Wollongong, Australia, in 2014.

He is currently a Research Fellow with ARC Centre of Excellence for Electromaterials Science, University of Wollongong, mainly focusing on soft robotics for prosthetic devices. His research interests include simulations and analysis of electromagnetics, simulations and analysis of biomechanics of small intestine, mechanics of viscoelastic materials, and active locomotion of wireless capsule endoscopy.

**Emre Sariyildiz** (S'11, M'16) received his first Ph.D. degree in Integrated Design Engineering from Keio University, Tokyo, Japan, in September 2014 and second Ph.D. degree in Control and Automation Engineering from Istanbul Technical University, Istanbul, Turkey, in February 2016.

He was a research fellow in the department of Biomedical Engineering and Singapore Institute for Neurotechnology (SINAPSE) at National University of Singapore, Singapore, between 2014 and 2017. Since April 2017, he has been Lecturer in the School of Mechanical, Materials, Mechatronic and Biomedical Engineering at University of Wollongong, NSW, Australia.

His main research interests are control theory, robotics, mechatronics and motion control.

**Marc in het Panhuis** is from Grevenbicht (Limburg, the Netherlands). He is a chemical engineer (Ingenieur, University of Twente, the Netherlands) and a physicist (PhD, University of Dublin, Trinity College, Ireland).

At present, he is a Professor of Materials Science in the School of Chemistry and a Chief Investigator in the Australian Research Council Centre of Excellence for Electromaterials Science at the University of Wollongong (Australia). His research activities are focused on tough hydrogels, Additive Manufacturing (3D/4D printing), edible/living electronics, soft robotics and 3D printed fins/surfboards for surfing. He is an Associate Editor for the Journal of Materials Chemistry B.

**Geoffrey M. Spinks** received his PhD from the University of Melbourne in 1990 for his work on the fracture behavior of unsaturated polyesters. He was appointed as Lecturer at the University of Wollongong (UOW) in December 1989 and currently holds the position of Senior Professor at UOW.

He has maintained a research interest in the mechanical behavior of polymers, especially actuator materials ('artificial muscles'). He has published more than 200 journal papers, including five papers in Science. As at December 2017, he had a total of 10300 citations and an "h-index" of 47. He has been actively involved in teaching and administration at UOW. He co-founded the Bachelor of Nanotechnology degree courses and has served as Discipline Advisor, research center Director and Associate Dean Research. He is currently the Challenge Leader of Manufacturing Innovation in UOW's Global Challenge program.

**Gursel Alici** received the Ph.D. degree in robotics from the Department of Engineering Science, Oxford University, Oxford, U.K., in 1994. He is currently a Senior Professor at the University of Wollongong, Wollongong, Australia, where he is the Head of the School of Mechanical, Materials. Mechatronic and Biomedical Engineering since 2011. His research interests are soft robotics, system dynamics and control, robotic drug delivery systems, novel actuation concepts for biomechatronic applications, robotic mechanisms and manipulation systems, soft and smart actuators and sensors, and medical robotics. He has published more than 300 refereed publications and delivered numerous invited seminars and keynote talks on his areas of research.

Dr. Alici was a Technical Editor of the IEEE/ASME Transactions on Mechatronics during 2008–2012. He is a Technical Editor of the IEEE Access, the first IEEE open access journal with interdisciplinary scope. He has served on the international program committee of numerous IEEE/ASME International Conferences on Robotics and Mechatronics. He was the General Chair of the 2013 IEEE/ASME International Conference on Advanced Intelligent Mechatronics held in Wollongong, Australia. He is the leader of Soft Robotics for Prosthetic Devices theme of the ARC Center of Excellence for Electromaterials Science. He received the Outstanding Contributions to Teaching and Learning Award in 2010, the Vice-Chancellor's Interdisciplinary Research Excellence Award in 2013, and Vice-Chancellor's Award for Research Supervision in 2018 from the University of Wollongong. He has held a visiting professorship position at Swiss Federal Institute of Technology, Lausanne (EPFL), City University of Hong Kong, and University of Science and Technology of China (USTC).